

Silver Nanoparticle Impregnated Porous Carbon as a Nonenzymatic Hydrogen Peroxide Sensor

Yi-Song Zou^{1‡}, Miao-Miao Jia^{1‡}, Jun-Qin Fan¹, Fa-Mei Qin¹, Jian-Guo Yu^{1*}, Yong-Nan Zhao²

¹ College of Environment and Chemical Engineering & State Key Laboratory of Hollow-Fiber Membrane Materials and Membrane Processes, Tianjin Polytechnic University, Tianjin, P.R. China

² School of Materials Science and Engineering, Tianjin Polytechnic University, Tianjin, P.R. China

*E-mail: hh_y1118@hotmail.com

‡the authors contribute equally to this work.

Received: 14 March 2016 / Accepted: 3 May 2016 / Published: 4 June 2016

In this work, a non-enzymatic hydrogen peroxide sensor has successfully been realized based on Ag nanoparticles doped carbon modified carbon paste electrode (AgNPs/C-CPE) in pH = 7 phosphate buffer solution (PBS). The Ag nanoparticles doped carbon composites (AgNPs/C) were synthesized by a simple one-step carbonization method using sucrose with AgNO₃ as the carbon precursor. AgNPs/C-CPE for electrochemical responds of hydrogen peroxide was explored by using cyclic voltammetry (CV) and amperometry. Besides, contents of AgNPs and pH values were optimized. The AgNPs/C-CPE containing 13.5 wt% AgNPs exhibits the highest electrocatalytic activity for the detection of hydrogen peroxide in pH = 7 PBS. At an applied potential of 0 V, the non-enzymatic sensor of hydrogen peroxide also showed a good linear relationship in a wide concentration range of 0.5–400 μM with a correlation coefficient of 0.9987, a detection limit of 0.3 μM at a signal-to noise ratio of 3, and a high sensitivity of 309.4 μA cm⁻² mM⁻¹. The amorphous carbon-supported AgNPs not only avoided the use of chemical reductants but also improved the electrocatalytic activity and stability of Ag NPs.

Keywords: Nano-silver, hydrogen peroxide determination, nonenzymatic sensor, sucrose, electrocatalysis

1. INTRODUCTION

In recent years, the determination of hydrogen peroxide has been a considerable increase of interest in the design and development of new methods. A rapid, accurate and reliable determination of hydrogen peroxide is an important topic in many fields including food industry [1, 2], pharmaceutical [3], clinical [2] and environmental analysis [4, 5].

Many techniques have been employed for this purpose, such as chemiluminescence [6], chromatography [7], titrimetry [8] and electrochemistry [9]. Among these methods, electrochemistry methods based on enzyme-based biosensors have also been developed extensively due to their simplicity, high sensitivity and selectivity [10-12]. However, there are several disadvantages for enzymes-based hydrogen peroxide biosensors, such as instability, high cost of enzymes, complicated immobilization procedures and limited lifetime [13]. To avoid these problems, a number of studies have been carried out to develop the nonenzymatic sensors with low detection limit and wide response range [14, 15].

Nowadays, metal nanoparticles (NPs), play an important role in improving nonenzymatic sensors performance. In recent years, Ag nanoparticles with the small particle diameter and the large specific surface area have been used as electrocatalysis of hydrogen peroxide [16, 17] and display a high electrocatalytic activity. But the size, shape and distribution of as-prepared AgNPs usually depend on the supporting materials. The composites structures contained the supporting materials and AgNPs have been successfully used as the determination of hydrogen peroxide, such as AgNPs/polydopamine, AgNPs/ionic liquid functionalized multiwalled carbon nanotube, AgNPs/vinyl polymer, AgNPs/graphene, etc.[16-22]. Besides, porous carbon have also been employed as catalyst supports of AgNPs due to their abundant porous structures and large internal surface[23].

Herein, an important consideration is the select of supporting materials, which can improve the dispersive property and decreasing size of AgNPs. For example, the amorphous carbon-supported silver nanoparticles for electrochemical nonenzymatic H_2O_2 sensing exhibited excellent catalytic activity with high sensitivity and low detection limit [24]. Mao [25] et al. introduced Core-shell structured Ag@C for direct electrochemistry and hydrogen peroxide biosensor applications. The core-shell structure of Ag@C enhanced the reproducibility and long-term stability for application in the fabrication of biosensors due to its direct electrochemistry and functionalized surface for efficient immobilization of bio-molecules.

In this paper, we have fabricated a rapid, nontoxic and inexpensive nonenzymatic hydrogen peroxide biosensor based on a simple synthetic route towards synthesis and stabilization of AgNPs using carbonization of sucrose, $AgNO_3$ and sodium citrate mixtures. Importantly, the as-synthesized AgNPs/carbon (AgNPs/C) nanocomposites exhibit excellent catalytic activity for electrocatalytic hydrogen peroxide reduction.

2. EXPERIMENTAL SECTION

2.1. Reagents and apparatus

Hydrogen peroxide solution (30 wt.%) was purchased from Sinopharm Chemical Reagent Co., Ltd (Shanghai, China). Silver nitrate, sodium citrate, HNO_3 , Na_2HPO_4 , and $NaH_2PO_4 \cdot 2H_2O$ were obtained from the Tianjin Chemical Reagent Plant (Tianjin, China) and used without further purification. Phosphate buffer solution (PBS) was prepared by mixing suitable amounts of 0.2 M NaH_2PO_4/Na_2HPO_4 . The concentration of H_2O_2 solution was standardized by titrate method with standard $KMnO_4$ (0.01 M). A fresh solution of H_2O_2 was prepared daily by a serial dilution of the

standardized H₂O₂ solution before the electrochemical measurements and stored at 4 ° C. Deionized water was used for the preparation of buffer and standard solution.

X-ray power diffraction (XRD) was used to confirm the presence of Ag phase. XRD patterns of the samples were collected on a Japan Rigaku D_{max} 2000 X-ray diffractometer with Cu K α radiation ($\lambda=0.154178\text{nm}$). The morphology of the AgNPs/C was obtained with Hitachi H-800 transmission electron microscopy (TEM). Infrared spectrum of the sample was recorded with Perkin-Elmer Spectrum One FTIR spectrophotometer in the 400-4000 cm⁻¹ region using a sample on the KBr plate.

2.2. Preparation of nano-silver doped carbon modified carbon paste electrode

AgNPs/C nanocomposites were synthesized via a carbonization of sucrose, AgNO₃ and sodium citrate mixtures. 51 mg of AgNO₃, 1.0 g of sucrose and 50 mg of sodium citrate were sequentially dissolved in 50 mL of HNO₃ aqueous solution (2 M) to form a clear solution. Then, the mixed solution was stirred and heated to 110 °C for 5 h, dried in a vacuum oven at 60 ° C for 12h. The products were obtained by the calcinations of dried mixture at 550 ° C for 4 h in N₂ atmosphere. In order to highlight the performance of AgNPs/C composite, the samples of different silver contents were obtained through adding different mass of AgNO₃.

The samples slurries were prepared by 80 wt.% active material, 10 wt.% carbon black and 10 wt.% paraffin wax together with an adequate amount of ethanol solvent with the ultrasonic for 0.5 h and then coated onto carbon paste electrode. The carbon paste electrode was dried at 120 ° C under vacuum for more than 10 h. The as-prepared electrode from AgNPs/C was denoted as AgNPs/C-CPE.

2.3. Electrochemical measurement

Electrochemical measurement was performed with a CHI660D electrochemical analyzer (Shanghai Chenhua Instruments Co., China) in a conventional three-electrode cell. The working electrodes were modified nano-silver doped carbon electrodes. Platinum wire was used as the counter electrode and a saturated calomel electrode (SCE) as the reference electrode. All potentials were measured and reported versus SCE. All electrochemical experiments were carried out at room temperature. 0.2 M phosphate buffer solution (PBS, pH = 7.0) was used as the supporting electrolyte for hydrogen peroxide determination, and moreover, purged with nitrogen for at least 15 min to remove oxygen prior to experiments. The detection limit (LOD) was calculated as three times the standard deviation of the blank solution (10 times)/slope of the analytical curve according to IUPAC recommendation [26].

3. RESULTS AND DISCUSSION

3.1. Characterizations of AgNPs/C

TEM was applied to study the morphologies of AgNPs/C nanocomposites. As shown in Fig. 1, a spherical morphology of the as-prepared AgNPs can be observed.

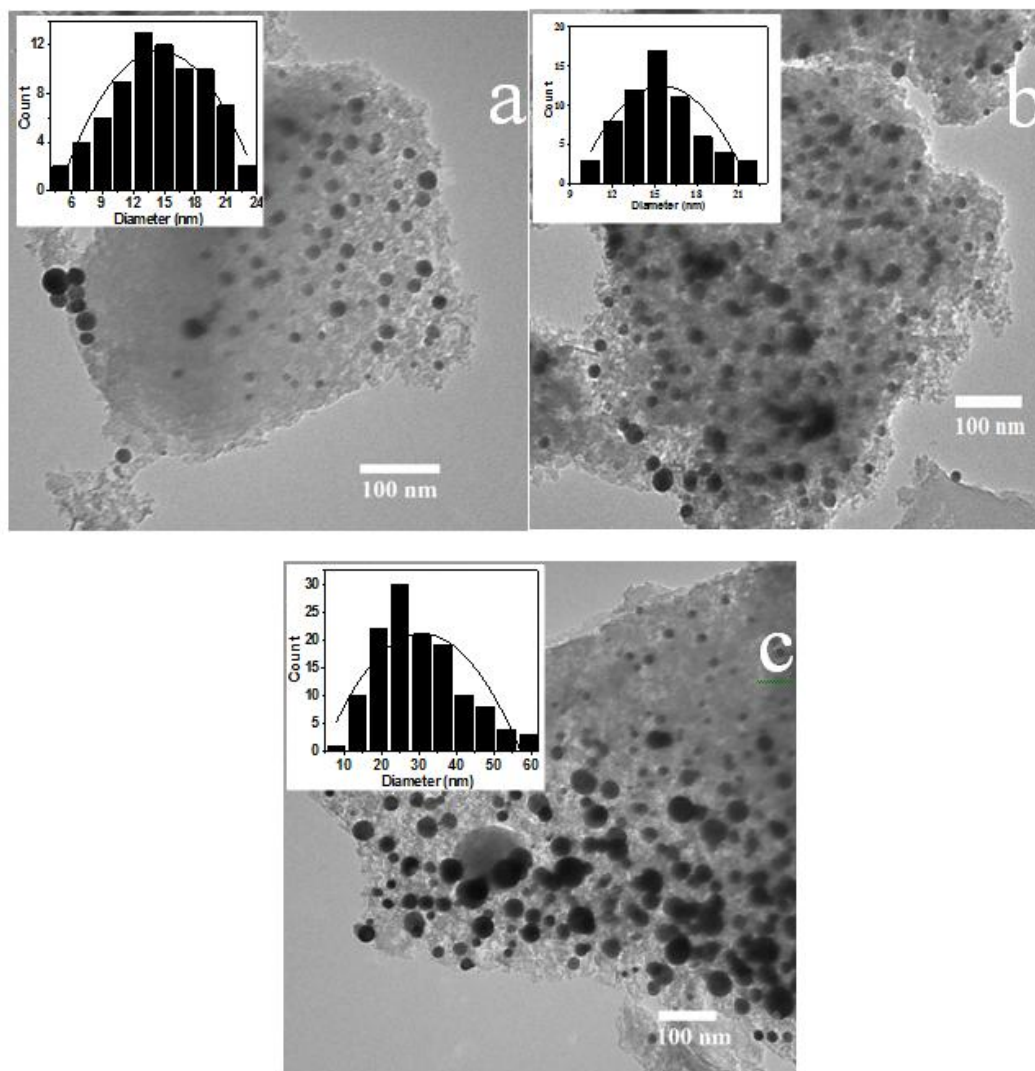


Figure 1. TEM image of AgNPs/C.

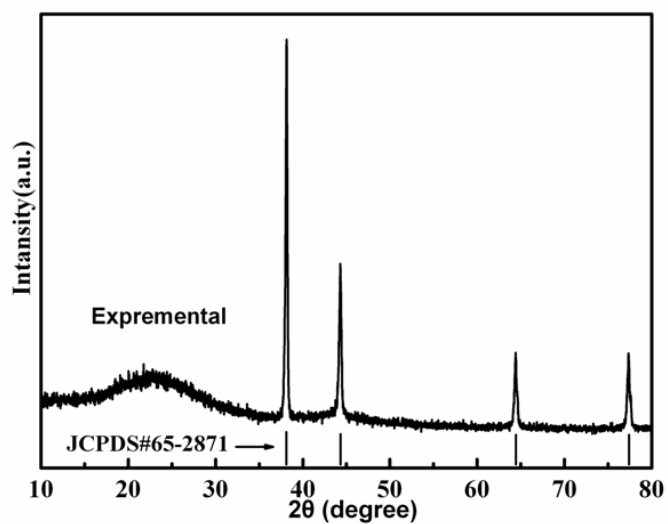


Figure 2. XRD patterns for the AgNPs/C composites.

The AgNPs are embedded in carbon matrix and highly dispersion. The inset in Fig. 1 shows that the average particle size of AgNPs with a narrow particle size distribution (9–29 nm) is 14 nm. With the increase of Ag content, the particle sizes of AgNPs are gradually enlarged (Fig. 1b and c). Moreover, the obvious agglomerations of AgNPs present when Ag content is high.

X-ray diffraction pattern of AgNPs/C nanocomposites was tested to identify the structure of the metal particles. In Fig. 2, the reflection peaks of AgNPs/C sample located at 38.1° , 44.3° , 64.4° and 77.5° are assigned to the (111), (200), (220) and (311) crystallographic planes of Ag metal, respectively. These peaks are well consistent with diffraction peaks of Ag in the standard Powder Diffraction File (JCPDS file No. 65-2871), indicating the formation of Ag metal. And the low intensity peak at 2θ values of nearly 24° is found the broad peak of amorphous carbon for the samples AgNPs/C.

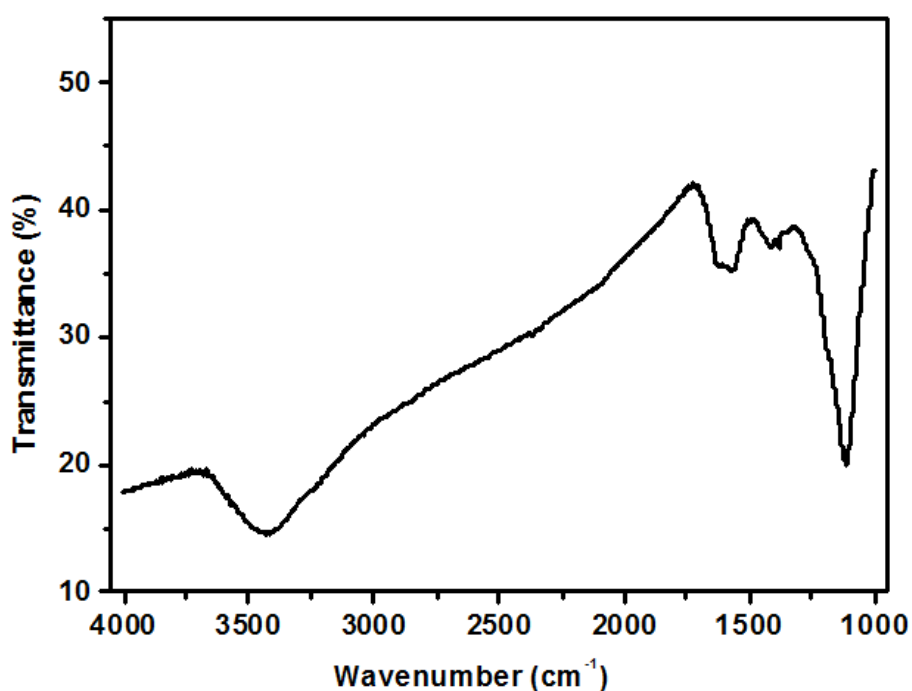


Figure 3. FTIR spectrum of the AgNPs/C sample.

The functional groups of AgNPs/C nanocomposites were characterized by FTIR spectrum. As shown in Fig. 3, the strong characteristic peak at 3438 cm^{-1} is attributed to the stretching vibration of O–H bond. Two wide peaks at $1633\text{--}1566$ and $1380\text{--}1421\text{ cm}^{-1}$ are attributed to stretching vibration of C=C. The strong absorption peak at 1110 cm^{-1} should be caused by the stretching vibration of C–O–C. The reaction of the surface Ag nanoparticles can be hindered due to the reaction of the active groups, such as C=C and C–O–C [27].

3.2. Effect of the ratio of Ag nanoparticles in carbon matrix

To optimize the electrocatalytic response of the AgNPs/C-CPE for hydrogen peroxide, the Ag-carbon mass ratios between 0 and 23.6 were studied for 1 mM hydrogen peroxide in 0.2 M PBS (pH =

7.0). Fig. 4 shows no obvious redox current peaks at carbon composite electrode without Ag nanoparticles present, however, the distinct increased redox current peaks appear at the electrodes with different contents of Ag, showing that Ag nanoparticles play an important role to accelerate the electron transfer and electrocatalytic behavior [27]. The oxidative peak potentials increase from 0.49 to 0.52 V and the reductive peak potentials decrease from 0.04 to -0.03 V for Ag-containing samples, exhibiting a similar redox potentials for reduction of hydrogen peroxide at silver nanoparticles embedded phosphomolybdate-polyaniline composite electrode [28].

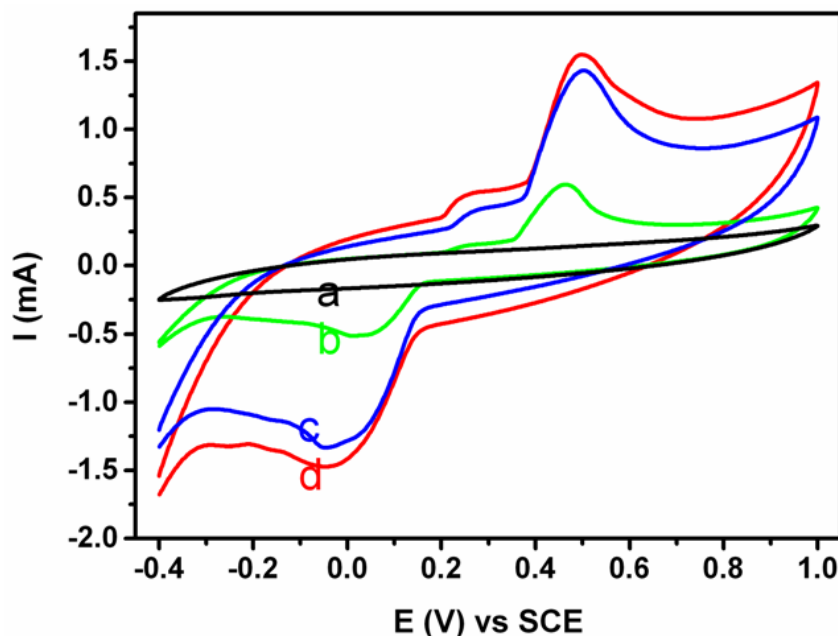


Figure 4. CVs of AgNPs/C-CPE with the different mass ratio (a: 0%, b: 5.3%, c: 14.5%, d: 23.6%) of Ag to carbon in 0.2 M PBS (pH = 7.0) N_2 saturated solution in the presence of 1.0 mM H_2O_2 (scan rate: 50 mV/s).

The largest peak currents of hydrogen peroxide are obtained at the Ag content of 14.5% in AgNPs/C composites, which is due to the agglomeration of Ag nanoparticles in largely Ag-carbon mass ratio and small contact surface in tiny Ag-carbon mass ratio, respectively. Thus, the Ag-doped carbon composites containing Ag of 14.5 wt. % is selected for hydrogen peroxide detection.

3.3. Cyclic voltammetric behaviors of hydrogen peroxide at AgNPs/C-CPE

The electrochemical response of hydrogen peroxide was investigated by cyclic voltammetry of AgNPs/C-CPE in a nitrogen saturated 0.2 M PBS (pH = 7.0) solution with and without 1 mM hydrogen peroxide. As shown in Fig. 5a, the CV curve of AgNPs/C-CPE exhibits the well-defined oxidation current peak at 0.45 V and reduction current peak at 0.05 V in the absence of 1 mM hydrogen peroxide, which are corresponded to the oxidation of Ag to Ag^+ and reduction of Ag^+ to Ag, respectively [29]. Besides, a weak oxidative current in the potential range of 0.21–0.35 V is induced by an oxidative reaction of as-prepared carbon composites with the oxygen-containing surface functional

groups [30]. However, Fig. 5b shows that the AgNPs/C-CPE exhibits significantly enhanced current signals in the presence of 1 mM hydrogen peroxide, indicating excellent catalytic ability of AgNPs/C-CPE to oxidation and reduction of hydrogen peroxide.

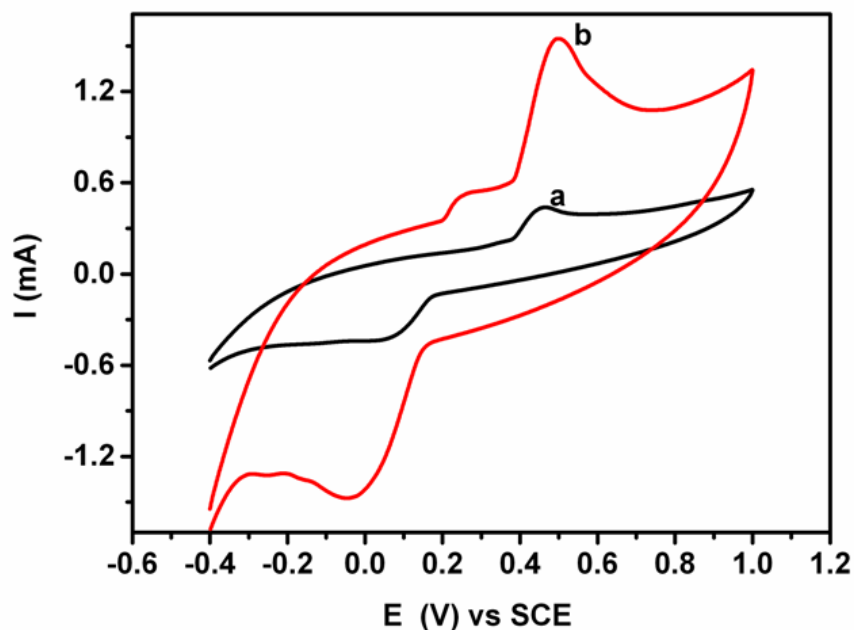


Figure 5. Cyclic voltammograms (CVs) of AgNPs/C-CPE modified GCE in N_2 saturated 0.2 M PBS (pH = 7.0) in the absence (a) and presence (b) of 1.0 mM H_2O_2 at a scan rate of 50 mV/s.

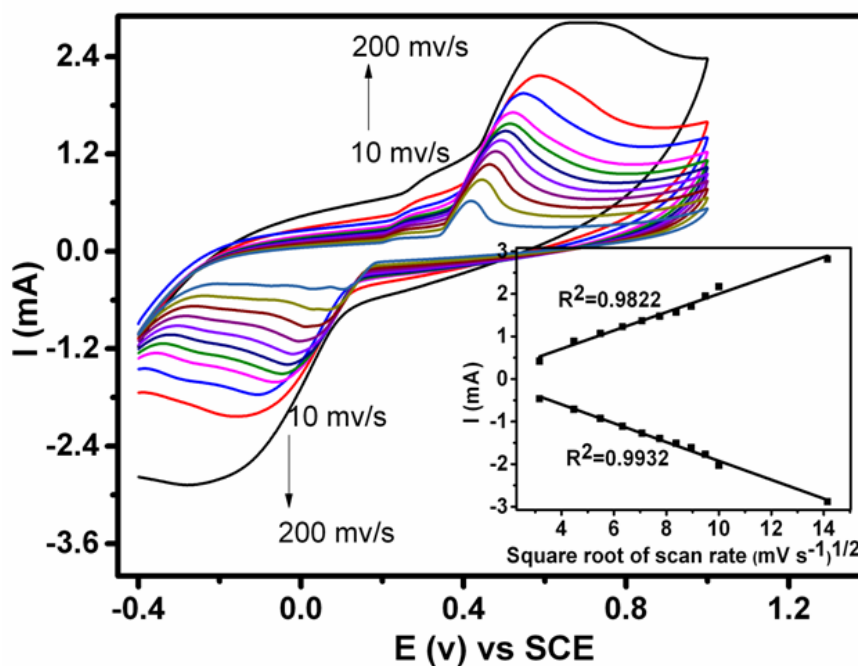


Figure 6. CVs of AgNPs/C-CPE in 1.0 mM H_2O_2 with 0.2 M PBS solution (pH = 7.0) at different scan rates (from 10 to 200 mV/s). *Inset:* plot of peak current H_2O_2 versus scan rate.

The direct electron transfer behavior between hydrogen peroxide and AgNPs/C-CPE was

explored by CV tests. As shown in Fig. 6, CV curves of the AgNPs/C-CPE shows well-defined peaks at different scan rates from 10mV/s to 200mV/s. With the increase of scan rate, the redox peak currents of the AgNPs/C-CPE increase accordingly. As shown in inset of Fig. 6, the well linear relations between redox peak currents and square roots of scan rates present, indicating a diffusion-controlled electrochemical process [31].

3.4. Amperometric response of the AgNPs/C-CPE to H_2O_2

To examine the amperometric responses of the as-prepared nano-silver doped carbon composites electrode, the successive detections of hydrogen peroxide were carried out in the stirring 0.2 M PBS solution. The oxidative potential of 0.4–0.8 V was abandoned because of the interferential oxidative current signals of ascorbic acid (AA), uric acid (UA) and dopamine (DA) (Fig. 7a). In Fig. 7b, no obvious reductive current signals of AA, UA and DA present at applied potential of 0 V. So the reduction potential of 0 V is used to determine amperometric responses of hydrogen peroxide.

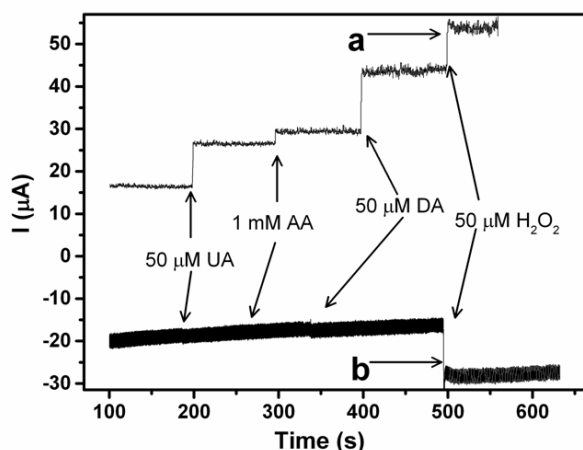


Figure 7. Current–time curves at applied potential of 0.48 V (A) and 0 V (B) for the AgNPs/C-CPE exposed to H_2O_2 (50 μ M), UA (50 μ M), DA (50 μ M), and AA (1 mM).

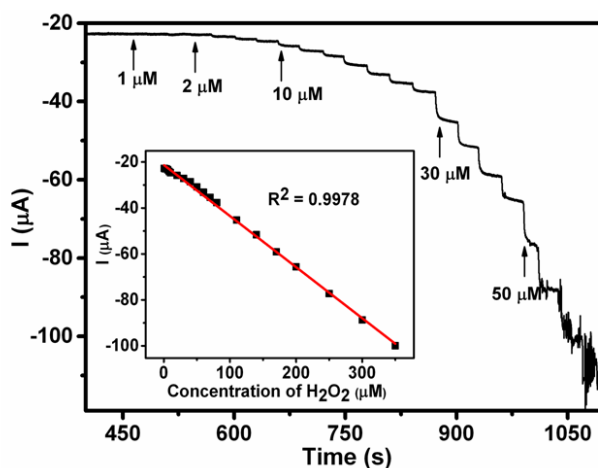


Figure 8. Steady-state response of AgNPs/C-CPE to successive injection of H_2O_2 into 0.2 M PBS N_2 saturated solution; *Inset* shows the calibration curve of the reduction currents vs. the concentrations of hydrogen peroxide.

The typical current-time curves for successive addition of hydrogen peroxide are displayed in Fig. 8. The current responds reach rapidly well-defined steady-state current within 3 s, indicating a fast amperometric response behavior. However, the current steps in Fig. 8 also showed a more electrocatalytic ability in the region of lower concentration of H₂O₂ due to the noises become more distinctly with increased concentration of H₂O₂. The inset in Fig. 8 shows the calibration curve of the sensor. With the addition of H₂O₂ into the stirring phosphate buffer solution, catalytic currents show linear response from 0.5 μM to 400 μM with a detection limit of 0.3 μM estimated at S/N = 3 and a sensitivity of 309.4 μA mM⁻¹ cm⁻². The regression equation is $I_p (\mu A) = -21.26 - 0.222C$ (C is the concentration of hydrogen peroxide in μM) with a correlation coefficient of 0.9978.

Table 1. Comparison of the performances using different electrodes for various nonenzymatic hydrogen peroxide sensors.

Electrode	LDR (μM)	LOD (μM)	Sensitivity (μA mM ⁻¹ cm ⁻²)	Stability	Reference
AgNPs/MWCNTs-IL	0.012-4.8	0.004	not reported	not reported	[18]
AgNPs-P(ABA)-Fe ₃ O ₄ /MCPE	0.005-5.5	1.74	not reported	94%/7 days	[21]
PSSN/GCE	0.04-2	0.040	not reported	81%/14 days	[22]
SWCNTs-PDA-AgNPs/GCE	50-175	0.6	335.6	not reported	[32]
Ag@TiO ₂ nanocomposite	0.83-43.3	0.83	65.2	98.5/21 days	[33]
AgNPs/Ox-pTTBA/MWCNT electrodes	10-260	0.24	not reported	95%/30 days	[34]
AgNPs/C	0.5-400	0.3	309.4	92.6%/30 days	This work

A comparison of this AgNPs/C with other hydrogen peroxide sensors contained AgNPs in the literature are shown in Table 1 in terms of linear detection range (LDR), limit of detection (LOD) and sensitivity. A broad linear range at AgNPs/C-CPE is better than those obtained on other electrodes reported recently. Therefore, the AgNPs/C-CPE can be used as a nonenzyme sensor for the detection of hydrogen peroxide with wide linear range, low LOD and high sensitivity.

3.5. Reproducibility and repeatability of AgNPs/C-CPE

The reproducibility of AgNPs/C-CPE was investigated by the peak current in response to 1 mM H₂O₂. The relative standard deviation (RSD) of the reductive peak current for the same electrode (5 times) was 2.7%, showing the good reproducibility at AgNPs/C-CPE. It still remained 98.7, 97.1 and 92.6% of its initial reductive current response to 1.0 mM H₂O₂ after the electrode was stored for 5, 10 and 30 day, respectively, suggesting the excellent stability at AgNPs/C-CPE compared with the other electrodes in Table 1.

4. CONCLUSIONS

In summary, the AgNPs/C nanocomposite were prepared by a facile method. The as-prepared nanocomposite has been demonstrated to be potential as a new type of H₂O₂ nonenzymatic sensor with an excellent electrocatalytic activity, especially a high sensitivity (309.4 $\mu\text{A mM}^{-1} \text{cm}^{-2}$), a low detection limit (0.3 μM) and a wide linear range (0.5–400 μM). The result showed that it is promising that such AgNPs/C nanocomposite sensor can be applied to detect hydrogen peroxide. In addition, the method can be further developed to prepare all kinds of metal doped carbon composite materials with a variety of application.

ACKNOWLEDGEMENTS

This research was supported by Nature Foundations of Tianjin (No. 14JCYBJC17500 and 15JCQNJC05700), National Students' Platform for Innovation and Entrepreneurship Training Program (No. 201410058053) and Nature Science Foundations of China (No. 21271138).

References

1. B. Zhang, Y. Cui, H. Chen, B. Liu, G. Chen, D. Tang, *Electroanal.*, 23 (2011) 1821.
2. D.N. Clausen, E.H. Duarte, E. R. Sartori, *Anal. Lett.*, 47 (2014):750.
3. S. Fathi, *Russ. J. Electrochem.*, 50 (2014) 468.
4. H. Song, Y. Ni, S. Kokot, *Biosens. Bioelectron.*, 56 (2014) 137.
5. H. Yang, M. Hua, S. Chen, R. Y. Tsai, *Biosens. Bioelectron.*, 41 (2013) 172.
6. L. Zhang, Y. Chen, Z. Zhang, L. Chao, *Sensor. Actuat. B-Chem.*, 193 (2014) 752.
7. U. Pinkernell, S. Effkemann, U. Karst, *Anal. Chem.*, 69 (1997) 3623.
8. N. V. Klassen, D. Marchington, H. C. E. McGowan, *Anal. Chem.*, 66 (1994) 2921.
9. K.-C. Lin, J.-J. Syu, S.-M. Chen, *Int. J. Electrochem. Sci.*, 10 (2015) 6886.
10. P. Sistani, A. Noori, M. F. Motlagh, A. H. Tamijani, E. Imani, Y. Shadram, R. Rahimzadeh, B. Ebrahimi, M. Sarebanhassanabadi, M. Negahdary, S. Majdi, *Int. J. Electrochem. Sci.*, 9 (2014) 3680.
11. B. Wang, X. Ji, H. Zhao, N. Wang, X. Li, R. Ni, Y. Liu, *Biosens. Bioelectron.*, 55 (2014) 113.
12. R. Ramachandran, S.-M. Chen, G. Gnana kumar, P. Gajendran, A. Xavier, N. B. Devi, *Int. J. Electrochem. Sci.*, 11 (2016) 1247.
13. G. Z. Zou, H. X. Ju, *Anal. Chem.*, 76 (2004) 6871.
14. J. Huang, Y. Zhu, H. Zhong, X. Yang, C. Li, *ACS Appl. Mater. Inter.*, 6 (2014) 7055.
15. J. Wang, Z. Wang, D. Zhao, C. Xu, *Anal. Chim. Acta*, 832 (2014) 34.
16. B. Zhan, C. Liu, H. Shi, C. Li, L. Wang, W. Huang, X. Dong, *Appl. Phys. Lett.*, 104 (2014) 243704.
17. F. Wang, R. Han, G. Liu, H. Chen, T. Ren, H. Yang, Y. Wen, *J. Electroanal. Chem.*, 706 (2013) 102.
18. X. Li, Y. Liu, L. Zheng, M. Dong, Z. Xue, X. Lu, X. Liu, *Electrochim. Acta*, 113 (2013) 170.
19. A. Moradi Golsheikh, N. M. Huang, H. N. Lim, R. Zakaria, C. Y. Yin, *Carbon*, 62 (2013) 405.
20. V. Pifferi, V. Marona, M. Longh, L. Falciola, *Electrochim. Acta*, 109 (2013) 447.
21. S. Chairam, W. Sroysee, C. Boonchit, C. Kaewprom, T. G. N. Wangnoi, M. Amatongchai, P. Jarujamrus, S. Tamaung, E. Somsook, *Int. J. Electrochem. Sci.*, 10 (2015) 4611.
22. J. Sophia, G. Muralidharan, *Sensor. Actuat. B-Chem.*, 193 (2014) 149.
23. S. Mao, Y. Long, W. Li, Y. Tu, A. Deng, *Biosens. Bioelectron.*, 48 (2013) 258.
24. D. Jiang, Y. Zhang, M. Huang, J. Liu, J. Wan, H. Chu, M. Chen, *J. Electroanal. Chem.*, 728 (2014) 26.
25. S. Mao, Y. Long, W. Li, Y. Tu, A. Deng, *Biosens. Bioelectron.*, 48 (2013) 258.

26. C. A. R. Salamanca-Neto, P. Hatumura, C. R. T. Tarly, E. R. Sartori, *Ionics*, 21 (2015) 1615.
27. Q. Wang, H. Niu, C. Mao, J. Song, S. Zhang, *Electrochim. Acta*, 127 (2014) 349.
28. A. Manivel, S. Anandan, *J. Solid State Electrochem.*, 15 (2011) 153.
29. S. Azizi, S. Ghasemi, S. Kaviani, *Biosens. Bioelectron.*, 62 (2014) 1.
30. Y. Liu, G. Yuan, Z. Jiang, Z. Yao, M. Yue, *Ionics*, 21 (2015) 801.
31. F. Li, Q. Zhang, D. Pan, M. Liu, Q. Kang, *Ionics*, 21 (2015) 1711.
32. Y. Lin, L. Li, L. Hu, Y. Xu, *Sensor. Actuat. B: Chem.*, 202 (2014) 527.
33. M. M. Khan, S. A. Ansari, J. Lee, M. H. Cho, *Mat. Sci. Eng. C-Mater.*, 33 (2013) 4692.
34. A. A. Abdelwahab, Y. B. Shim, *Sensor. Actuat. B-Chem.*, 201 (2014) 51.

© 2016 The Authors. Published by ESG (www.electrochemsci.org). This article is an open access article distributed under the terms and conditions of the Creative Commons Attribution license (<http://creativecommons.org/licenses/by/4.0/>).